better than those of oxides produced in our laboratory from $N_2O + SiH_4$ mixtures, but may be substantially improved by low-temperature annealing.*

The resistivity, measured at a field strength of 1 MV/cm, was found to be a strong function of deposition temperature only, and the variation is shown in Fig. 2. A temperature of approximately 200°C was required to optimise the resistivity, which then has a value of around $5 \times 10^{14}\,\Omega$cm. This is a reasonable value, lying in the usually quoted range for SiO_2 of 10^{14}–$10^{16}\,\Omega$cm.[11] Films deposited at 150°C and below were very leaky and contained many pinholes, and so are of little use for device applications.

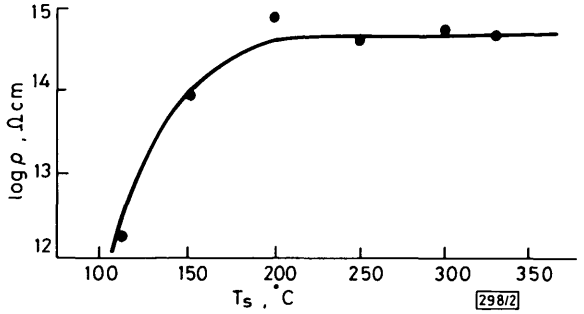

Fig. 2 *Variation of resistivity with T_s*

The dielectric strength was also found to depend only on the deposition temperature. For deposition temperatures below about 150°C, breakdown was observed at fields of 2–4 MV/cm, but high-temperature films gave values typically in the range 6·5–8·5 MV/cm.

Discussion: Thin films of SiO_2 with good properties have been deposited from $NO + SiH_4$ mixtures. The use of such mixtures as an alternative to conventional $N_2O + SiH_4$ mixtures will now be discussed.

Using N_2O to produce SiO_2 by PECVD requires careful control of the deposition conditions, with a very large N_2O/SiH_4 ratio usually required (up to 60:1[1,3]). This is necessary as, although N_2O has a relatively low dissociation energy (1·74 eV), there is also a large associated activation barrier. NO has a large dissociation energy (6·54 eV), but has the advantage of being able to react directly with SiH_2 and SiH_3 radicals in the plasma (for instance $SiH_3 + NO \rightarrow H_3SiON$), and this reduces the dependence of film composition on the plasma conditions. It was thought that the gas phase reactions could lead to particulate formation, but this was not observed.

The fact that oxidation proceeds by a different path when NO is used (compared to N_2O) is illustrated by the IR and RI results. Although the ratio of oxygen/silicon atoms in the input gas is the same (under the same deposition conditions) for $NO + SiH_4$ and $N_2O + SiH_4$ plasmas, the film composition differs markedly. The $NO + SiH_4$ plasma always leads to highly oxidised films under all deposition conditions, whereas the use of low powers or gas ratios with N_2O results in the principal IR peak being shifted to wavenumbers as low as $1010\,cm^{-1}$ and values of RI in excess of 1·54.[10]

To conclude, it has been demonstrated that it is possible to produce thin films of SiO_2 from the glow discharge decomposition of silane and nitric oxide. These films generally have properties comparable to other PECVD oxides, but have a slightly more porous structure. They have the advantage of being relatively insensitive to deposition conditions, but a potential disadvantage is that NO is toxic with a TLV of 25 parts in 10^6.

Acknowledgments: One of the authors (DJE) acknowledges the financial support of the UK SERC.

D. J. EAGLE
W. I. MILNE

University Engineering Department
Trumpington Street
Cambridge CB2 1PZ, United Kingdom

4th September 1986

References

1 VAN DEN VEN, E. P. G. T.: *Solid State Technol.*, 1981, **24**, p. 167

* EAGLE, D. J.: unpublished results

2 GOROWITZ, B., GORCZYCA, T. B., and SAIA, R. J.: *ibid.*, 1985, **28**, p. 197

3 DAUTREMONT-SMITH, W. C., and LOPTA, J.: *J. Vac. Sci & Technol. B*, 1983, **1**, p. 943

4 ADAMS, A. C., ALEXANDER, F. B., CAPIO, C. D., and SMITH, T. E.: *J. Electrochem. Soc.*, 1981, **128**, p. 1545

5 REINBERG, A. R.: *J. Electron. Mater.*, 1979, **8**, p. 345

6 EAGLE, D. J., and MILNE, W. I.: *Thin Solid Films*, to be published

7 MUKHARJEE, S. P., and EVANS, P. E.: *ibid.*, 1972, **14**, p. 105

8 KIRK, R. W.: *in* HOLLAHAN, J. R., and BELL, A. T. (Eds.): 'Techniques & applications of plasma chemistry' (Wiley Interscience, 1974, p. 347

9 LONGEWAY, P. A., ESTES, R. D., and WEAKLIEM, H. A.: *J. Phys. Chem.*, 1984, **88**, p. 73

10 EAGLE, D. J., MILNE, W. I., and BARDEN, P. E.: Proceedings of EMS conference, Strasbourg, 1986, to be published

11 SZE, S. M.: 'Physics of semiconductor devices' (John Wiley, 1981)

CHARACTERISTICS OF SEPARATED-GATE JFETs

Indexing terms: Semiconductor devices and materials, Junction structures, FETs

In the subthreshold region of JFETs a reach-through diode is formed between the top and bottom gates. This has consequences for the application of separated-gate JFETs.

Introduction: The past few years have witnessed the appearance of both bipolar and MOS silicon processes in which junction FETs are integrated. Generally the JFET channel is sandwiched between two gates which are physically and thus also electrically joined; hence the term 'joined-gate JFET'. Furthermore, a 'separated-gate' JFET has been introduced in the form of a ring-gate structure with, in the centre, the drain surrounded by a ring-shaped top gate which thus may be totally embedded in the channel region. This structure is also attractive in high-frequency bipolar processes, since a high JFET cutoff frequency may be achieved by fixing the epitaxial bottom gate voltage and thus eliminating the epi-substrate capacitance.[1–3] Furthermore, such a separated-gate JFET is feasible in simple processes where the substrate must form the bottom gate.[1,4] A SPICE model for separated-gate JFETs has been proposed by Das,[4] where in particular a MOS-like bulk effect is accounted for. Hitherto, however, another significant difference between the joined- and separated-gate JFETs has been overlooked: the double diode structure from top to bottom gate forms a reach-through diode which may conduct current when the separated-gate JFET is functioning in the subthreshold mode of operation. This letter demonstrates that it is nevertheless possible to exploit the advantages of separated-gate JFETs, if the region of operation is well controlled. Additionally, the special characteristics of the reach-through diode make it an attractive device for voltage limiting functions, for example.

Experimental: Experiments were performed on *p*- and *n*-channel JFETs produced in a double-implantation bipolar

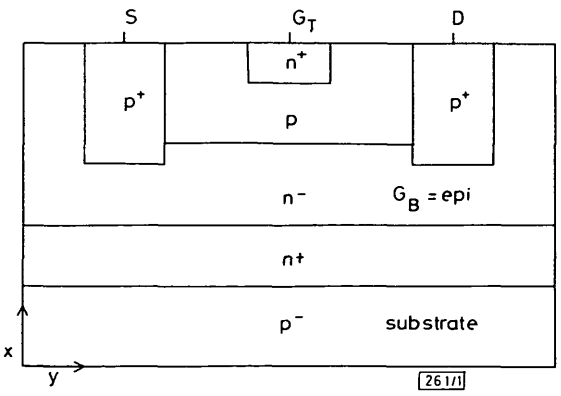

Fig. 1 *Basic structure of p-channel JFET*

process. Results are reported here for measurements on the p-channel JFETs, for which the top gate and channel region are implanted into an epitaxial n-layer, forming the bottom gate (see Fig. 1). Different pinch-off voltages are achieved by varying the channel implantation dose and energy. The devices have a length $L = 2\,\mu m$ and width $W = 430\,\mu m$. All voltages are referred to the source voltage.

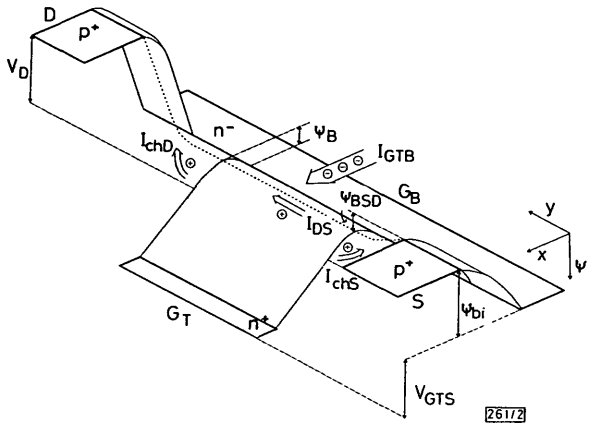

Fig. 2 *Potential distribution Ψ throughout the JFET, when $V_{GTS} \neq V_{GBS} = 0$ and $V_{GTS} > V_{PTo}$*
Main electron and hole currents are indicated

Reach-through diode from top to bottom gate: The top-gate/channel/bottom-gate double diode of the JFET is an n^+pn structure which may function as an asymmetrical reach-through diode.[5] Fig. 2 shows a potential diagram of the total JFET structure. For a fixed bottom gate voltage V_{GBS} and the top gate voltage $V_{GTS} \geq V_{GBS}$, the potential barrier Ψ_B at the channel-epi reverse-biased diode may be reduced by increasing V_{GTS} pas the point where the channel is completely depleted. Electrons may then be injected over the barrier, and the current density will increase as $\exp(-q|\Psi_B|/kT)$.[5] Thus if Ψ_B is directly proportional to V_{GTS}, the top to bottom gate current I_{GTB} will increase exponentially with V_{GTS}. This is empirically verified for modulation of Ψ_B by the top gate, which forms an abrupt junction diode with the channel region. The lightly doped bottom gate, however, gives a much less efficient modulation of the potential barrier formed at the reverse-biased top-gate/channel diode. This effect is obvious in Fig. 3, which displays an example of typical reach-through diode characteristics, and may also be appreciated by studying Fig. 4. Fig. 3 also illustrates that I_{GTB} is not influenced by the reverse-biasing of the gate-channel diodes.

Correlation of JFET characteristics: The reach-through diode current I_{GTB} is related to the JFET characteristics in the manner shown in Fig. 4. First, consider the case where one of the gates is set at 0 V. If $V_{GBS} = 0$ the pinch-off voltage, denoted V_{PTo}, is extracted by an extrapolation of the quadratic behaviour of $I_{DS}(V_{GTS})$ in the saturation region, and likewise for $V_{GTS} = 0$, the pinch-off voltage V_{PBo} is determined from $I_{DS}(V_{GBS})$. Beyond the pinch-off voltage the JFET functions in the subthreshold (exponential) mode, where the hole current I_{DS} is injected over the potential barrier Ψ_{BSD} (see Fig. 2).[6] In the transition region between the quadratic and exponential modes of operation, the channel becomes totally depleted and I_{GTB} is initiated. From the measured graphs it is clear that I_{GTB} is solely a function of $(V_{GTS} - V_{GBS})$. Furthermore, the voltage span in which $I_{GTB} = 0$ is equal to $(V_{PTo} + V_{PBo})$. At the drain/source ends of the channel the reverse-biasing should result in some increase of the potential barrier Ψ_B, but apparently for this given device length this has no significant influence on I_{GTB}. On the other hand, the pinch-off voltage is dependent on the voltage alloted to the fixed gate. Thus, as is illustrated in Fig. 4*a* for $V_{GBS} \geq 1$ V, pinch-off may be achieved before the onset of I_{GTB} if the fixed gate voltage is sufficiently high.

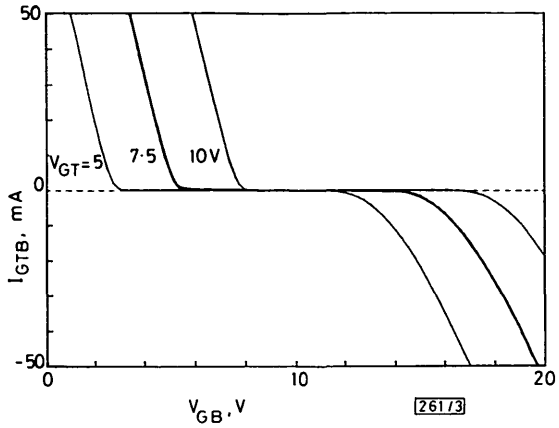

Fig. 3 *Reach-through diode characteristics for device JF3 in Table 1*

Effect on source-drain current: The drain current I_D is initially unperturbed by I_{GTB}, which is to be expected in view of the fact that the former is a hole current and the latter an electron current. However, at a given I_{GTB} level an increase in I_D is observed. This is in accordance with the fact that, above a certain value of the electric field, the electrons may gain enough energy to excite electron-hole pairs by impact ionisation.[5] The holes will consequently be swept from the channel to either the source or drain contact (see currents I_{chS}, I_{chD} in

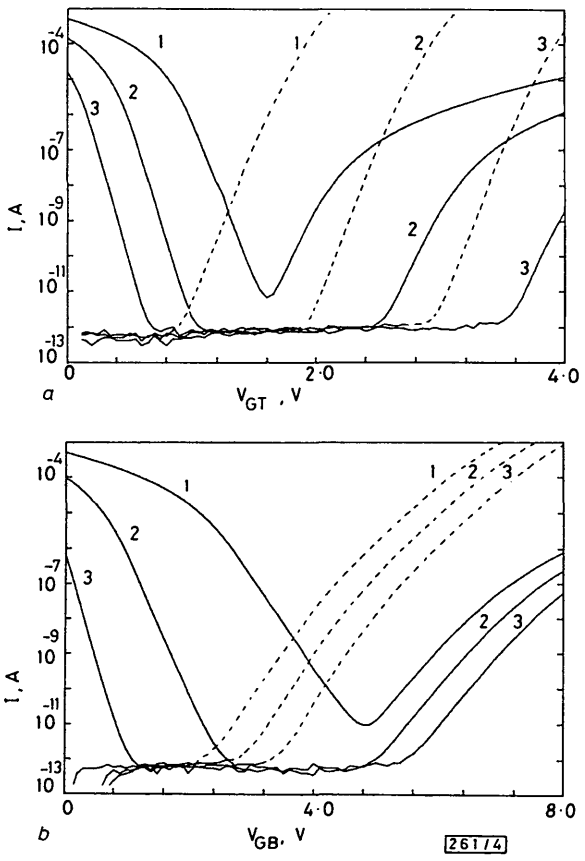

Fig. 4 *Currents I_D (solid curves) and I_{GTB} (broken curves) in device JF3 in Table 1*
a Against the gate voltage V_{GTS} with V_{GBS} fixed at (1) 0 V, (2) 1 V and (3) 2 V
b Against V_{GBS} with V_{GTS} fixed at (1) 0 V, (2) 0·5 V and (3) 1 V

Table 1

Device	Channel dose	Implant energy	V_{PTo}	V_{PBo}	$I_{GTB}(V_o)$
	cm^{-2}	keV	V	V	A
JF1	5×10^{12}	150	subthreshold	subthreshold	5×10^{-4}
JF2	$7{\cdot}5 \times 10^{12}$	125	0·96	1·77	3×10^{-7}
JF3	10^{13}	125	2·89	9·50	3×10^{-11}

Fig. 2). The probability of creating holes by impact ionisation should increase with increasing channel depth, i.e. increasing pinch-off voltage. This is confirmed in Table 1, where, for different channel implantations, I_{GTB} is given at the voltage V_o where the I_{GTB} induced drain current appears.

Conclusion: The reach-through diode current and the associated impact ionisation currents, all fundamental features of every separated-gate JFET, must be taken into consideration when substituting these JFETs in circuit functions normally confined to joined-gate JFETs. For high pinch-off voltages devices operating continuously in the quadratic mode, problems may perhaps only be encountered in the form of unpredicted currents in a start-up situation or in overdrive conditions. However, as soon as the subthreshold region is involved, it will generally be compulsory to choose the biasing conditions such that I_{GTB} is eliminated. This is in particular true for low-current devices designed such that the channel is always depleted. In these cases, choosing $V_{GBS} = 0$ will normally not be acceptable, and characterisation of the devices including I_{GTE}, I_{chS} and I_{chD} is imperative. The reach-through diode in itself is an interesting device, offering a design versatility not available in normal diodes.

Acknowledgment: This work is supported by the Foundation for Fundamental Research on Matter (FOM).

L. K. NANVER
E. J. G. GOUDENA

Department of Electrical Engineering
Delft University of Technology
Mekelweg 4
2628 CD Delft, The Netherlands

27th August 1986

References

1 MEIJER, G. C. M., and VERWEIJEN, F. L. J.: 'JFETs fabricated in a standard IC process for bipolar transistors', *IEEE J. Solid-State Circuits*, 1978, **SC-13**, pp. 530–532
2 LUI, S. K., and MEYER, R. G.: 'A high-frequency bipolar JFET I^2L process', *IEEE Trans.*, 1982, **ED-29**, pp. 1319–1323
3 MALHI, S. D. S., and SALAMA, C. A. T.: 'Double-implanted subvolt JFETs', *Solid-State Electron.*, 1982, **25**, pp. 791–795
4 DAS, C.: 'Realizatie en modelleren van ionen-geimplanteerde junktie-veldeffekttransistoren in kompatibele processen'. Thesis, Katholieke Universiteit, Leuven, Belgium, 1984
5 SZE, S. M.: 'Physics of semiconductor devices' (Wiley, 1981, 2nd edn.)
6 BREWER, R. J.: 'The 'barrier mode' behavior of a junction FET at low drain currents', *Solid-State Electron.*, 1975, **18**, pp. 1013–1017

ANALYSIS OF MULTIPLE-QUANTUM-WELL DISTRIBUTED FEEDBACK LASER

Indexing term: Semiconductor lasers

The doping and detuning dependences of the threshold, dynamic and spectral properties of multiple-quantum-well distributed feedback lasers were analysed theoretically. It was shown that optimised detuning improves the dynamic and spectral properties. It was also shown that donor doping significantly reduces the threshold current and spectral linewidth.

The detuning effect, i.e. adjusting the lasing wavelength to shorter than the gain peak, has been shown to improve the dynamic and spectral properties of distributed feedback (DFB) lasers.[1,2] On the other hand, multiple-quantum-well (MQW) lasers were also reported to theoretically improve,[3] and the increase of the relaxation oscillation frequency was confirmed experimentally.[4] However, it is not clear how the dynamic and spectral properties of MQW lasers are affected by detuning, since the band structure and the gain spectrum is different from that of double-heterostructure (DH) lasers. In addition, it was also predicted recently that the doping of acceptors in MQW lasers increases the relaxation oscillation frequency.[5] In this letter we describe the theoretical effect of detuning and doping on various characteristics of MQW-DFB lasers.

For the calculation of gain, we used the model which takes account of intraband relaxation time,[6] and only TE modes were considered. For the calculation of quantised energy levels, coupling between wells was neglected. In addition, we took into account the bandgap shrinkage ΔE_g phenomenologically as

$$\Delta E_g = -1{\cdot}3 \times 10^{-8}(n^{1/3} + p^{1/3}) \quad (1)$$

where n and p are the carrier density of electrons and holes, respectively, in units of cm^{-1}. This expression was chosen to fit the experimental data[7] (33 meV for $n = p = 2 \times 10^{18}\,cm^{-3}$). The threshold current density J_{th}, linewidth enhancement factor α and spontaneous emission factor n_{sp} were obtained by the same manner as in Reference 3.

Since we are considering DFB lasers, the lasing wavelength can be chosen independent of the gain peak, and the threshold carrier density was calculated such that the gain at a given wavelength equals the threshold gain. The cavity loss was assumed to be $42\,cm^{-1}$, which corresponds to a coupling coefficient of $100\,cm^{-1}$ and a cavity length of $300\,\mu m$, and $10\,cm^{-1}$ was used for the internal absorption loss. We take a case of five 10 nm GaAs wells and four $Al_{0.2}Ga_{0.8}As$ barrier layers, whose confinement factor is estimated to be 0·15.[3] The intraband relaxation time τ_{in} is assumed to be 0·2 ps.[3]

The dependence of the threshold current and the differential gain dg/dn on the lasing wavelength (photon energy) is shown in the upper half of Fig. 1. Owing to the highly asymmetric gain spectrum of the MQW structure, the threshold current density increases much faster in the lower-energy side than in the higher-energy side. The relaxation oscillation frequency is a measure to estimate the maximum limit of direct current modulation, and is proportional to the square root of the differential gain. Unlike conventional DH-DFB lasers, the band-filling effect is smaller than the bandgap shrinkage effect in MQW lasers, so the differential gain reaches a maximum value with relatively small detuning, and then decreases at higher photon energies. The spectral linewidth $\Delta\nu$ is proportional to $(1 + \alpha^2)n_{sp}$.[8]

The photon energy dependence of α, n_{sp} and $(1 + \alpha^2)n_{sp}$ is depicted in the lower half of Fig. 1. α decreases and n_{sp} increases with increasing photon energy, so $(1 + \alpha^2)n_{sp}$ shows a complicated dependence. In this case, by detuning the lasing wavelength by about 10 nm shorter than the gain peak, the linewidth decreases by about 30%. However, the optimum dutuning and the degree of improvement depends on device parameters such as the well width and well number.

The effect of doping on the threshold current, differential gain and the linewidth is shown in Fig. 2. For the calculation,

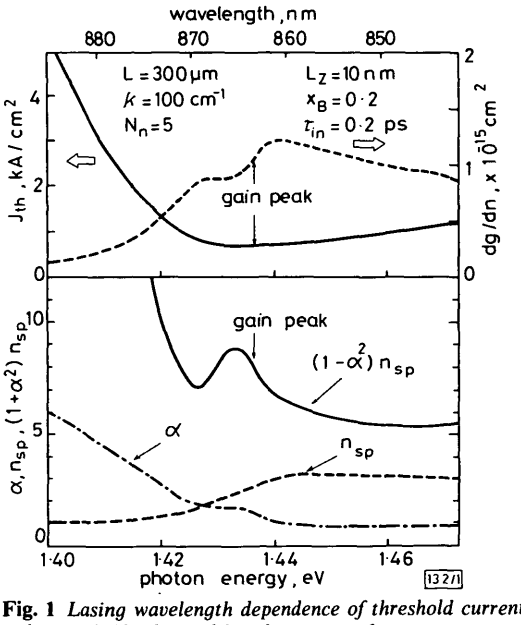

Fig. 1 *Lasing wavelength dependence of threshold current J_{th}, differential gain dg/dn, linewidth enhancement factor α, spontaneous emission factor n_{sp} and $(1 + \alpha^2)n_{sp}$*